

Search for Second and Third Generation Leptoquarks Including Production via Technicolor Interactions in $p\bar{p}$ collisions at $\sqrt{s} = 1.8$ TeV

T. Affolder,²¹ H. Akimoto,⁴³ A. Akopian,³⁶ M. G. Albrow,¹⁰ P. Amaral,⁷ S. R. Amendolia,³² D. Amidei,²⁴ K. Anikeev,²² J. Antos,¹ G. Apollinari,¹⁰ T. Arisawa,⁴³ T. Asakawa,⁴¹ W. Ashmanskas,⁷ M. Atac,¹⁰ F. Azfar,²⁹ P. Azzi-Bacchetta,³⁰ N. Bacchetta,³⁰ M. W. Bailey,²⁶ S. Bailey,¹⁴ P. de Barbaro,³⁵ A. Barbaro-Galtieri,²¹ V. E. Barnes,³⁴ B. A. Barnett,¹⁷ M. Barone,¹² G. Bauer,²² F. Bedeschi,³² S. Belforte,⁴⁰ G. Bellettini,³² J. Bellinger,⁴⁴ D. Benjamin,⁹ J. Bensinger,⁴ A. Beretvas,¹⁰ J. P. Berge,¹⁰ J. Berryhill,⁷ B. Bevensee,³¹ A. Bhatti,³⁶ M. Binkley,¹⁰ D. Bisello,³⁰ R. E. Blair,² C. Blocker,⁴ K. Bloom,²⁴ B. Blumenfeld,¹⁷ S. R. Blusk,³⁵ A. Bocci,³² A. Bodek,³⁵ W. Bokhari,³¹ G. Bolla,³⁴ Y. Bonushkin,⁵ D. Bortoletto,³⁴ J. Boudreau,³³ A. Brandl,²⁶ S. van den Brink,¹⁷ C. Bromberg,²⁵ M. Brozovic,⁹ N. Bruner,²⁶ E. Buckley-Geer,¹⁰ J. Budagov,⁸ H. S. Budd,³⁵ K. Burkett,¹⁴ G. Busetto,³⁰ A. Byon-Wagner,¹⁰ K. L. Byrum,² P. Calafiura,²¹ M. Campbell,²⁴ W. Carithers,²¹ J. Carlson,²⁴ D. Carlsmith,⁴⁴ J. Cassada,³⁵ A. Castro,³⁰ D. Cauz,⁴⁰ A. Cerri,³² A. W. Chan,¹ P. S. Chang,¹ P. T. Chang,¹ J. Chapman,²⁴ C. Chen,³¹ Y. C. Chen,¹ M. -T. Cheng,¹ M. Chertok,³⁸ G. Chiarelli,³² I. Chirikov-Zorin,⁸ G. Chlachidze,⁸ F. Chlebana,¹⁰ L. Christofek,¹⁶ M. L. Chu,¹ C. I. Ciobanu,²⁷ A. G. Clark,¹³ A. Connolly,²¹ J. Conway,³⁷ J. Cooper,¹⁰ M. Cordelli,¹² J. Cranshaw,³⁹ D. Cronin-Hennessy,⁹ R. Cropp,²³ R. Culbertson,⁷ D. Dagenhart,⁴² F. DeJongh,¹⁰ S. Dell'Agnello,¹² M. Dell'Orso,³² R. Demina,¹⁰ L. Demortier,³⁶ M. Deninno,³ P. F. Derwent,¹⁰ T. Devlin,³⁷ J. R. Dittmann,¹⁰ S. Donati,³² J. Done,³⁸ T. Dorigo,¹⁴ N. Eddy,¹⁶ K. Einsweiler,²¹ J. E. Elias,¹⁰ E. Engels, Jr.,³³ W. Erdmann,¹⁰ D. Errede,¹⁶ S. Errede,¹⁶ Q. Fan,³⁵ R. G. Feild,⁴⁵ C. Ferretti,³² R. D. Field,¹¹ I. Fiori,³ B. Flaughner,¹⁰ G. W. Foster,¹⁰ M. Franklin,¹⁴ J. Freeman,¹⁰ J. Friedman,²² Y. Fukui,²⁰ S. Galeotti,³² M. Gallinaro,³⁶ T. Gao,³¹ M. Garcia-Sciveres,²¹ A. F. Garfinkel,³⁴ P. Gatti,³⁰ C. Gay,⁴⁵ S. Geer,¹⁰ D. W. Gerdes,²⁴ P. Giannetti,³² P. Giromini,¹² V. Glagolev,⁸ M. Gold,²⁶ J. Goldstein,¹⁰ A. Gordon,¹⁴ A. T. Goshaw,⁹ Y. Gotra,³³ K. Goulios,³⁶ C. Green,³⁴ L. Groer,³⁷ C. Grosso-Pilcher,⁷ M. Guenther,³⁴ G. Guillian,²⁴ J. Guimaraes da Costa,¹⁴ R. S. Guo,¹ R. M. Haas,¹¹ C. Haber,²¹ E. Hafen,²² S. R. Hahn,¹⁰ C. Hall,¹⁴ T. Handa,¹⁵ R. Handler,⁴⁴ W. Hao,³⁹ F. Happacher,¹² K. Hara,⁴¹ A. D. Hardman,³⁴ R. M. Harris,¹⁰ F. Hartmann,¹⁸ K. Hatakeyama,³⁶ J. Hauser,⁵ J. Heinrich,³¹ A. Heiss,¹⁸ M. Herndon,¹⁷ B. Hinrichsen,²³ K. D. Hoffman,³⁴ C. Holck,³¹ R. Hollebeek,³¹ L. Holloway,¹⁶ R. Hughes,²⁷ J. Huston,²⁵ J. Huth,¹⁴ H. Ikeda,⁴¹ J. Incandela,¹⁰ G. Introzzi,³² J. Iwai,⁴³ Y. Iwata,¹⁵ E. James,²⁴ H. Jensen,¹⁰ M. Jones,³¹ U. Joshi,¹⁰ H. Kambara,¹³ T. Kamon,³⁸ T. Kaneko,⁴¹ K. Karr,⁴² H. Kasha,⁴⁵ Y. Kato,²⁸ T. A. Keaffaber,³⁴ K. Kelley,²² M. Kelly,²⁴ R. D. Kennedy,¹⁰ R. Kephart,¹⁰ D. Khazins,⁹ T. Kikuchi,⁴¹ B. Kilminster,³⁵ M. Kirby,⁹ M. Kirk,⁴ B. J. Kim,¹⁹ D. H. Kim,¹⁹ H. S. Kim,¹⁶ M. J. Kim,¹⁹ S. H. Kim,⁴¹ Y. K. Kim,²¹ L. Kirsch,⁴ S. Klimenko,¹¹ P. Koehn,²⁷ A. Köngeter,¹⁸ K. Kondo,⁴³ J. Konigsberg,¹¹ K. Kordas,²³ A. Korn,²² A. Korytov,¹¹ E. Kovacs,² J. Kroll,³¹ M. Kruse,³⁵ S. E. Kuhlmann,² K. Kurino,¹⁵ T. Kuwabara,⁴¹ A. T. Laasanen,³⁴ N. Lai,⁷ S. Lami,³⁶ S. Lammel,¹⁰ J. I. Lamoureux,⁴ M. Lancaster,²¹ G. Latino,³² T. LeCompte,² A. M. Lee IV,⁹ K. Lee,³⁹ S. Leone,³² J. D. Lewis,¹⁰ M. Lindgren,⁵ T. M. Liss,¹⁶ J. B. Liu,³⁵ Y. C. Liu,¹ N. Lockyer,³¹ J. Loken,²⁹ M. Loretto,³⁰ D. Lucchesi,³⁰ P. Lukens,¹⁰ S. Lusin,⁴⁴ L. Lyons,²⁹ J. Lys,²¹ R. Madrak,¹⁴ K. Maeshima,¹⁰ P. Maksimovic,¹⁴ L. Malferrari,³ M. Mangano,³² M. Mariotti,³⁰ G. Martignon,³⁰ A. Martin,⁴⁵ J. A. J. Matthews,²⁶ J. Mayer,²³ P. Mazzanti,³ K. S. McFarland,³⁵ P. McIntyre,³⁸ E. McKigney,³¹ M. Menguzzato,³⁰ A. Menzione,³² C. Mesropian,³⁶ T. Miao,¹⁰ R. Miller,²⁵ J. S. Miller,²⁴ H. Minato,⁴¹ S. Miscetti,¹² M. Mishina,²⁰ G. Mitselmakher,¹¹ N. Moggi,³ E. Moore,²⁶ R. Moore,²⁴ Y. Morita,²⁰ A. Mukherjee,¹⁰ T. Muller,¹⁸ A. Munar,³² P. Murat,¹⁰ S. Murgia,²⁵ M. Musy,⁴⁰ J. Nachtman,⁵ S. Nahn,⁴⁵ H. Nakada,⁴¹ T. Nakaya,⁷ I. Nakano,¹⁵ C. Nelson,¹⁰ D. Neuberger,¹⁸ C. Newman-Holmes,¹⁰ C.-Y. P. Ngan,²² P. Nicolaidi,⁴⁰ H. Niu,⁴ L. Nodulman,² A. Nomerotski,¹¹ S. H. Oh,⁹ T. Ohmoto,¹⁵ T. Ohsugi,¹⁵ R. Oishi,⁴¹ T. Okusawa,²⁸ J. Olsen,⁴⁴ W. Orestes,²¹ C. Pagliarone,³² F. Palmonari,³² R. Paoletti,³² V. Papadimitriou,³⁹ S. P. Pappas,⁴⁵ D. Partos,⁴ J. Patrick,¹⁰ G. Pauletta,⁴⁰ M. Paulini,²¹ C. Paus,²² L. Pescara,³⁰ T. J. Phillips,⁹ G. Piacentino,³² K. T. Pitts,¹⁶ R. Plunkett,¹⁰ A. Pompos,³⁴ L. Pondrom,⁴⁴ G. Pope,³³ M. Popovic,²³ F. Prokoshin,⁸ J. Proudfoot,² F. Ptohos,¹² O. Pukhov,⁸ G. Punzi,³² K. Ragan,²³ A. Rakitine,²² D. Reher,²¹ A. Reichold,²⁹ W. Riegler,¹⁴ A. Ribon,³⁰ F. Rimondi,³ L. Ristori,³² W. J. Robertson,⁹ A. Robinson,²³ T. Rodrigo,⁶ S. Rolli,⁴² L. Rosenson,²² R. Roser,¹⁰ R. Rossin,³⁰ W. K. Sakumoto,³⁵ D. Saltzberg,⁵ A. Sansoni,¹² L. Santi,⁴⁰ H. Sato,⁴¹ P. Savard,²³ P. Schlabach,¹⁰ E. E. Schmidt,¹⁰ M. P. Schmidt,⁴⁵ M. Schmitt,¹⁴ L. Scodellaro,³⁰ A. Scott,⁵ A. Scribano,³² S. Segler,¹⁰ S. Seidel,²⁶ Y. Seiya,⁴¹ A. Semenov,⁸ F. Semeria,³ T. Shah,²² M. D. Shapiro,²¹ P. F. Shepard,³³ T. Shibayama,⁴¹ M. Shimojima,⁴¹ M. Shochet,⁷ J. Siegrist,²¹ G. Signorelli,³² A. Sill,³⁹ P. Sinervo,²³ P. Singh,¹⁶ A. J. Slaughter,⁴⁵ K. Sliwa,⁴² C. Smith,¹⁷ F. D. Snider,¹⁰ A. Solodsky,³⁶ J. Spalding,¹⁰ T. Speer,¹³ P. Sphicas,²² F. Spinella,³² M. Spiropulu,¹⁴ L. Spiegel,¹⁰ J. Steele,⁴⁴ A. Stefanini,³² J. Strologas,¹⁶ F. Strumia,¹³ D. Stuart,¹⁰ K. Sumorok,²² T. Suzuki,⁴¹ T. Takano,²⁸ R. Takashima,¹⁵ K. Takikawa,⁴¹ P. Tamburello,⁹ M. Tanaka,⁴¹ B. Tannenbaum,⁵ W. Taylor,²³ M. Tecchio,²⁴ P. K. Teng,¹ K. Terashi,⁴¹ S. Tether,²² D. Theriot,¹⁰ R. Thurman-Keup,² P. Tipton,³⁵ S. Tkaczyk,¹⁰ K. Tollefson,³⁵ A. Tollestrup,¹⁰ H. Toyoda,²⁸ W. Trischuk,²³ J. F. de Troconiz,¹⁴ J. Tseng,²²

N. Turini,³² F. Ukegawa,⁴¹ T. Vaiculis,³⁵ J. Valls,³⁷ S. Vejcek III,¹⁰ G. Velev,¹⁰ R. Vidal,¹⁰ R. Vilar,⁶ I. Volobouev,²¹ D. Vucinic,²² R. G. Wagner,² R. L. Wagner,¹⁰ J. Wahl,⁷ N. B. Wallace,³⁷ A. M. Walsh,³⁷ C. Wang,⁹ C. H. Wang,¹ M. J. Wang,¹ T. Watanabe,⁴¹ D. Waters,²⁹ T. Watts,³⁷ R. Webb,³⁸ H. Wenzel,¹⁸ W. C. Wester III,¹⁰ A. B. Wicklund,² E. Wicklund,¹⁰ H. H. Williams,³¹ P. Wilson,¹⁰ B. L. Winer,²⁷ D. Winn,²⁴ S. Wolbers,¹⁰ D. Wolinski,²⁴ J. Wolinski,²⁵ S. Wolinski,²⁴ S. Worm,²⁶ X. Wu,¹³ J. Wyss,³² A. Yagil,¹⁰ W. Yao,²¹ G. P. Yeh,¹⁰ P. Yeh,¹ J. Yoh,¹⁰ C. Yosef,²⁵ T. Yoshida,²⁸ I. Yu,¹⁹ S. Yu,³¹ Z. Yu,⁴⁵ A. Zanetti,⁴⁰ F. Zetti,²¹ and S. Zucchelli³

(CDF Collaboration)

- ¹ *Institute of Physics, Academia Sinica, Taipei, Taiwan 11529, Republic of China*
- ² *Argonne National Laboratory, Argonne, Illinois 60439*
- ³ *Istituto Nazionale di Fisica Nucleare, University of Bologna, I-40127 Bologna, Italy*
- ⁴ *Brandeis University, Waltham, Massachusetts 02254*
- ⁵ *University of California at Los Angeles, Los Angeles, California 90024*
- ⁶ *Instituto de Fisica de Cantabria, University of Cantabria, 39005 Santander, Spain*
- ⁷ *Enrico Fermi Institute, University of Chicago, Chicago, Illinois 60637*
- ⁸ *Joint Institute for Nuclear Research, RU-141980 Dubna, Russia*
- ⁹ *Duke University, Durham, North Carolina 27708*
- ¹⁰ *Fermi National Accelerator Laboratory, Batavia, Illinois 60510*
- ¹¹ *University of Florida, Gainesville, Florida 32611*
- ¹² *Laboratori Nazionali di Frascati, Istituto Nazionale di Fisica Nucleare, I-00044 Frascati, Italy*
- ¹³ *University of Geneva, CH-1211 Geneva 4, Switzerland*
- ¹⁴ *Harvard University, Cambridge, Massachusetts 02138*
- ¹⁵ *Hiroshima University, Higashi-Hiroshima 724, Japan*
- ¹⁶ *University of Illinois, Urbana, Illinois 61801*
- ¹⁷ *The Johns Hopkins University, Baltimore, Maryland 21218*
- ¹⁸ *Institut für Experimentelle Kernphysik, Universität Karlsruhe, 76128 Karlsruhe, Germany*
- ¹⁹ *Korean Hadron Collider Laboratory: Kyungpook National University, Taegu 702-701; Seoul National University, Seoul 151-742; and SungKyunKwan University, Suwon 440-746; Korea*
- ²⁰ *High Energy Accelerator Research Organization (KEK), Tsukuba, Ibaraki 305, Japan*
- ²¹ *Ernest Orlando Lawrence Berkeley National Laboratory, Berkeley, California 94720*
- ²² *Massachusetts Institute of Technology, Cambridge, Massachusetts 02139*
- ²³ *Institute of Particle Physics: McGill University, Montreal H3A 2T8; and University of Toronto, Toronto M5S 1A7; Canada*
- ²⁴ *University of Michigan, Ann Arbor, Michigan 48109*
- ²⁵ *Michigan State University, East Lansing, Michigan 48824*
- ²⁶ *University of New Mexico, Albuquerque, New Mexico 87131*
- ²⁷ *The Ohio State University, Columbus, Ohio 43210*
- ²⁸ *Osaka City University, Osaka 588, Japan*
- ²⁹ *University of Oxford, Oxford OX1 3RH, United Kingdom*
- ³⁰ *Università di Padova, Istituto Nazionale di Fisica Nucleare, Sezione di Padova, I-35131 Padova, Italy*
- ³¹ *University of Pennsylvania, Philadelphia, Pennsylvania 19104*
- ³² *Istituto Nazionale di Fisica Nucleare, University and Scuola Normale Superiore of Pisa, I-56100 Pisa, Italy*
- ³³ *University of Pittsburgh, Pittsburgh, Pennsylvania 15260*
- ³⁴ *Purdue University, West Lafayette, Indiana 47907*
- ³⁵ *University of Rochester, Rochester, New York 14627*
- ³⁶ *Rockefeller University, New York, New York 10021*
- ³⁷ *Rutgers University, Piscataway, New Jersey 08855*
- ³⁸ *Texas A&M University, College Station, Texas 77843*
- ³⁹ *Texas Tech University, Lubbock, Texas 79409*
- ⁴⁰ *Istituto Nazionale di Fisica Nucleare, University of Trieste/ Udine, Italy*
- ⁴¹ *University of Tsukuba, Tsukuba, Ibaraki 305, Japan*
- ⁴² *Tufts University, Medford, Massachusetts 02155*
- ⁴³ *Waseda University, Tokyo 169, Japan*
- ⁴⁴ *University of Wisconsin, Madison, Wisconsin 53706*
- ⁴⁵ *Yale University, New Haven, Connecticut 06520*

We report the results of a search for second and third generation leptoquarks using 88 pb^{-1} of data recorded by the Collider Detector at Fermilab. Color triplet technipions, which play the role of scalar leptoquarks, are investigated due to their potential production in decays of strongly coupled color octet technirhos. Events with a signature of two heavy flavor jets and missing energy may indicate the decay of a second (third) generation leptoquark to a charm (bottom) quark and a neutrino. As the data is found to be consistent with Standard Model expectations, mass limits are determined.

PACS: 14.80.Ly, 13.85.Rm

While limited to interactions via gauge bosons in the Standard Model, quarks and leptons couple directly in theories with leptoquarks [1–6]. The leptoquarks found in various models generally share similar characteristics. They appear as color triplet bosons allowing for a Yukawa coupling of strength λ between quarks and leptons. In order to avoid the constraints of proton decay, the interactions are assumed to conserve baryon and lepton number. In addition, leptoquarks are typically assumed to couple to fermions of the same generation in order to suppress flavor changing neutral currents (FCNCs) [7]. The principal mechanisms for leptoquark pair production at the Tevatron are $q\bar{q}$ annihilation and gluon fusion through either direct coupling to the gluon (“continuum”) or a technicolor resonance state.

The characteristics of leptoquark production from continuum can be categorized according to spin. For scalar leptoquarks, the production cross section is parameter free since the coupling between leptoquark and gluon is determined by the gauge symmetries of quantum chromodynamics (QCD) [8]. Those interactions involving quark-lepton-leptoquark vertices are neglected due to the assumed small relative value of λ . The scalar leptoquark production cross section is known to next-to-leading order [9]. Vector leptoquark interactions include anomalous couplings to the gluons denoted as κ_G and λ_G which are related to the anomalous ‘magnetic’ moment and the ‘electric’ quadrupole moment in the color field [10]. κ_G and λ_G are associated with different gauge fields and are considered independent in order to reduce the reliance on any one specific model. Probing the conspicuous choices leads to the investigation of Yang-Mills type coupling when $\kappa_G = \lambda_G = 0$ and minimal coupling when $\kappa_G = 1$ and $\lambda_G = 0$. At present only leading order processes have been calculated for vector leptoquark pair production [10]. The phenomenological parameter β describes the branching fraction of a leptoquark decaying to a final state which includes a charged lepton. Previous CDF analyses have examined $\beta = 1$ and excluded leptoquark masses at the 95% confidence level (CL) for the second generation with scalar coupling of $202 \text{ GeV}/c^2$ and for the third generation with scalar coupling of $99 \text{ GeV}/c^2$, minimal vector coupling of $170 \text{ GeV}/c^2$, and Yang-Mills coupling of $225 \text{ GeV}/c^2$ [11]. For $\beta = 0$, a search conducted by the D0 Collaboration has set limits at the 95% CL for second generation leptoquarks of 79, 160, and $205 \text{ GeV}/c^2$ [12] and for third generation leptoquarks of 94, 148, and $216 \text{ GeV}/c^2$ [13] for scalar, minimal coupling, and Yang-Mills coupling, respectively.

Enhancement of leptoquark pair production occurs through the decay of technicolor resonance states. Obviating the need for elementary scalar bosons, technicolor theories present a dynamical explanation for electroweak symmetry breaking in which quark and lepton chiral symmetries are explicitly broken by gauge interactions including extended technicolor with a coupling constant that evolves slowly to suppress FCNCs [3–5]. In one of the established formulations, a complete family of technifermions composed of an isodoublet of color triplet techniquarks and an isodoublet of color singlet technileptons form a rich spectrum of technimesons [4]. Combinations of techniquarks form color octet

technirhos, ρ_{T8} , some of which are endowed with the same quantum numbers as the gluon allowing for s -channel coupling. The color triplet and octet technipions, denoted by π_{LQ} and π_{T8} , couple in a Higgs-like fashion to quarks and leptons and thus are expected to decay into heavy fermion pairs. The π_{LQ} is identified as a scalar leptoquark. Contingent on phase space, the ρ_{T8} may decay to quark, gluon, π_{LQ} , or π_{T8} pairs. The leading-order cross section for leptoquark pair production from technirho resonance depends upon the technirho and leptoquark masses and the technirho width [5]. The technirho width is sensitive to changes in mass difference between the color octet technipion and leptoquark, $\Delta M = M(\pi_{T8}) - M(\pi_{LQ})$. QCD corrections can be calculated to find an expected mass difference of $50 \text{ GeV}/c^2$ [5]. For the restricted case $M(\rho_{T8}) < 2M(\pi_{LQ})$, a previous CDF analysis of the dijet mass spectrum has already excluded $260 < M(\rho_{T8}) < 480 \text{ GeV}/c^2$ at the 95% CL [14]. CDF has also conducted a search when decay to π_{LQ} is kinematically allowed for third generation leptoquark production using the $\tau\bar{\tau}b\bar{b}$ channel [15].

The decay modes to $c\bar{\nu}$ and $b\bar{\nu}$ corresponding to $\beta = 0$ are utilized to search for pair produced leptoquarks in events with two heavy flavor jets, missing transverse energy, and the absence of high transverse momentum leptons. The continuum leptoquarks are assumed to be strictly second and third generation, their decays involving ν_μ and ν_τ respectively. Of the several potential color triplet technipion decays, the modes $\pi_{LQ} \rightarrow c\bar{\nu}_\tau$ for $M(\pi_{LQ})$ less than the top quark mass and $\pi_{LQ} \rightarrow b\bar{\nu}_\tau$ are possible. Technically, the color triplet technipion decaying to $c\bar{\nu}_\tau$ is a leptoquark of mixed generation. Yet since neutrino types cannot be distinguished in detector events, these are considered to be similar to the second generation leptoquark. Questions concerning potential FCNC contributions arising from this will not be addressed in the present work.

These signatures can be employed to conduct a search for leptoquark particles at CDF using a total integrated luminosity of $88.0 \pm 3.6 \text{ pb}^{-1}$ collected during the 1994-1995 Tevatron run. Since detailed descriptions of the CDF detector and its components exist [16], only a recapitulation follows. Detector positions are given by a coordinate system with the z axis along the beamline, azimuthal angle, ϕ , in the plane transverse to the z axis, and pseudorapidity, η . Nearest to the interaction point, the silicon vertex detector (SVX') consists of four layers providing impact parameter measurements with respect to the primary vertex in the plane transverse to the beam direction [17]. The primary vertices along the beam direction are reconstructed by the vertex tracking chamber in the region $|\eta| < 3.25$. Directly inside a 1.4 T superconducting solenoidal magnet encompassing a range $|\eta| < 1.1$ rests the central drift chamber used for precision measurements of charged particles' transverse momenta. The calorimeter consists of electromagnetic and hadronic components covering a range $|\eta| < 4.2$. The muon system covers a range of $|\eta| < 1$. Missing transverse energy, \cancel{E}_T , indicating the presence of neutrinos in the process, is the energy needed to balance the raw energy deposited in the calorimeter towers with $|\eta| < 3.6$ in the plane transverse to the beam direction.

Various selection criteria are applied to the data sample collected using a trigger requiring $\cancel{E}_T > 35 \text{ GeV}$. Once the irrelevant sources of \cancel{E}_T originating from accelerator induced and cosmic ray effects are removed, the remaining 304582 events are dominated by multijet QCD background. Calorimeter information is used to determine jets through a fixed cone algorithm [18] where the cone radius is 0.4 in $\eta - \phi$ space. The raw energy deposited in the calorimeter towers is used to find the jet energies. Events characterized by two or three hard jets with $E_T \geq 15 \text{ GeV}$ and $|\eta| \leq 2$ and no additional jets with $E_T > 7 \text{ GeV}$ and $|\eta| \leq 3.6$ are selected. These requirements reduce both the background from $t\bar{t}$ events which typically results in four or more hard jets and the soft QCD background arising from gluon radiation. To reduce systematic effects due to the trigger threshold, the \cancel{E}_T trigger requirement is increased to $\cancel{E}_T > 40 \text{ GeV}$. As jet energy mismeasurement results in missing energy appearing parallel or anti-parallel to the jet direction, the \cancel{E}_T direction is required to be well separated from any jet. To implement these criteria, the angles between \cancel{E}_T and any jet are restricted to $\Delta\phi(\cancel{E}_T, j) > 45^\circ$ and between \cancel{E}_T and the leading E_T jet $\Delta\phi(\cancel{E}_T, j_1) < 165^\circ$. To further reduce QCD background, the angle between the two highest E_T jets is restricted to $45^\circ < \Delta\phi(j_1, j_2) < 165^\circ$. 569

events pass these selections. The W and Z backgrounds are lessened by rejecting events containing loosely identified, high transverse momentum leptons (excluding tau). Electron candidates are required to have lateral and longitudinal shower profiles consistent with an electron [19], $E_T < 2 \cdot p_T$ when the momentum measurement is available, and $E_T > 10$ GeV. Muon candidates are determined by matching a charged track to the calorimeter energy deposition compatible with a minimum ionizing particle [19]. If identified in the muon chambers, the muon candidates must have $p_T > 10$ GeV/c, otherwise they must have $p_T > 15$ GeV/c with additional E_T as measured by the calorimeter less than 5 GeV in a 0.4 radius cone around the lepton. Once these criteria are employed, 396 events remain.

The technique of tagging c and b jets found in the recent CDF scalar top and bottom quarks search [20] using the jet probability algorithm [21] is employed. The algorithm uses precision SVX' information to identify long-lived heavy quarks. Jet probability, \mathcal{P}_{jet} , is derived from the combination of probabilities that individual tracks come from a primary vertex (track probability) for all tracks associated with a particular jet. The algorithm constructs the probability that an ensemble of tracks in a jet originates from a primary vertex. For jets arising from primary vertices, \mathcal{P}_{jet} is flat from 0 to 1. When the jets emerge from secondary vertices, \mathcal{P}_{jet} peaks at 0. Events corresponding to leptoquark decays with a charm quark in the final state use the requirement of at least one taggable jet with $\mathcal{P}_{jet} \leq 0.05$. For the signatures with a bottom quark, at least one taggable jet with $\mathcal{P}_{jet} \leq 0.01$ must be present. Applying these criteria, 11 observed events for the c and 5 observed events for the b tagged data samples are found. The signal tagging efficiency is approximately 27% for second generation leptoquarks and 49% for third generation leptoquarks.

After the jet probability requirements are satisfied, the predominant background is determined to come from non-QCD sources. Events with W and one jet, where the W decays leptonically to a tau that decays hadronically, compose the largest single background with 7.6 and 3.0 expected background events for $\mathcal{P}_{jet} \leq 0.05$ and 0.01, respectively. The total expected $W/Z/t\bar{t}$ /diboson background for the 0.05 jet probability cut is 11.1 and for the 0.01 cut is 4.5. The QCD background comprises an expected 3.4 events for $\mathcal{P}_{jet} \leq 0.05$ and 1.3 events for $\mathcal{P}_{jet} \leq 0.01$. Since the same data set and techniques are being employed as in reference [20], further discussion concerning backgrounds can be found there.

Several Monte Carlo generators are employed together with a CDF detector simulation package to both estimate the backgrounds and the expected signal. The VECBOS program [22] allows for the tree-level calculation of a vector boson plus jets production at the parton level. The partons are then fragmented and hadronized using HERWIG routines [23]. Vector boson pair production and decay are simulated in ISAJET [24]. HERWIG [23] is employed to compute $t\bar{t}$ events. To generate the signal events for scalar leptoquarks from continuum, PYTHIA version 5.7 [25] is used which already possesses the proper production cross section. For the vector leptoquarks, PYTHIA is encoded with the relevant cross section for leading order vector leptoquark production including anomalous couplings as derived in [10]. For the technicolor produced leptoquarks, the expected signal is generated by incorporating the cross sections and widths appropriate for color triplet technipion production [5] into PYTHIA. The parton distribution function employed in all these simulations was CTEQ 4L [26]. The renormalization scale for scalar leptoquark simulations was $\mu = M(LQ)$, for vector leptoquark simulations $\mu = \sqrt{\hat{s}}$, and for technicolor simulations $\mu = M(\pi_{LQ})$. The same search criteria are applied to the Monte Carlo samples as was to the data.

Reflective of typical values, efficiencies for second generation leptoquarks produced from continuum are approximately 5% for $M(LQ) = 125$ GeV/c², whereas in the case of production from technirho decay efficiencies between 3 and 7% are found, the efficiencies decreasing as the technirho mass increases from 400 to 700 GeV/c². Third generation leptoquarks with $M(LQ) = 150$ GeV/c² are found with approximately 10% efficiency for continuum and as the technirho mass varies from 300 to 800 GeV/c², the efficiency decreases from 12 to 3%. Since relative differences

in efficiency between scalar and vector continuum produced leptoquarks are less than 5% for $M(LQ) > 140 \text{ GeV}/c^2$, the scalar leptoquark efficiency is employed for both. The signal efficiency is degraded by a factor of 0.93 to account for the effect of multiple $p\bar{p}$ interactions not present in the simulations [20].

The systematic uncertainties for tagging efficiency, jet energy scale, trigger, luminosity, and multiple interactions from [20] are applicable to both the continuum and technicolor produced leptoquark analyses and combine for an uncertainty of 18%. Only those uncertainties which are unique to leptoquarks will be mentioned below. The dominant source of systematic uncertainty for continuum leptoquarks comes from gluon radiation in the initial (ISR) and final (FSR) state. The systematic uncertainty was determined to be 31% by comparing efficiencies obtained with ISR or FSR neglected to those where ISR and FSR were included. The effect of different choices of parton distribution function and QCD renormalization scale is found to give a systematic uncertainty in efficiency of 10%. Combining these results with those of [20], the maximum total systematic uncertainty for the efficiency is 37%. For the leptoquarks generated from technirho decay, the systematic uncertainty due to ISR and FSR is found to be 25%. The choice of parton distribution function and variation due to the renormalization scale set to $\mu = M(\pi_{LQ})/2$ and $2M(\pi_{LQ})$ contribute a 9% and 20% systematic uncertainty, respectively, to both the efficiencies and cross sections. Consolidating the various results for the technicolor case, a maximum total systematic uncertainty of 37% is likewise established.

For the second generation leptoquark search, 11 observed events are found and a background of 14.5 ± 4.2 events is estimated. In the case of third generation leptoquarks, 5 observed events are found and a background of 5.8 ± 1.8 events is estimated. As no excess of observed events over Standard Model background was found, 95% CL limits are determined through a background subtraction method [27] to ascertain excluded regions of parameter space.

For the continuum, a 95% CL limit on scalar and vector leptoquark production cross sections for the various leptoquark types and masses are determined. The results are shown in Figure 1. In the case of second generation leptoquarks, when these values are compared to their corresponding theoretical cross sections [9,10] scalar leptoquarks with $M < 123 \text{ GeV}/c^2$, minimally coupled vector leptoquarks with $M < 171 \text{ GeV}/c^2$, and Yang-Mills vector leptoquarks with $M < 222 \text{ GeV}/c^2$ are excluded. Similarly, in the case of third generation leptoquarks, scalar leptoquarks with $M < 148 \text{ GeV}/c^2$, minimally coupled vector leptoquarks with $M < 199 \text{ GeV}/c^2$, and Yang-Mills vector leptoquarks with $M < 250 \text{ GeV}/c^2$ are excluded.

The technicolor produced scalar leptoquarks entail a complication in that the technirho mass is an additional parameter. Furthermore, since the production cross section is affected by the mass difference ΔM , the values $\Delta M = 0$, $50 \text{ GeV}/c^2$, and ∞ are probed. The 95% CL exclusion regions in the $M(\rho_{T8}) - M(\pi_{LQ})$ plane shown as shaded areas in Figures 2 and 3 are determined by comparing the 95% CL cross section limit for production of leptoquarks which decay to quarks and neutrinos to theoretical predictions [5]. The kinematically forbidden region is given by $M(\rho_{T8}) < 2M(\pi_{LQ})$. The continuum scalar leptoquark limits found earlier in this analysis set an excluded mass for second generation leptoquarks below $123 \text{ GeV}/c^2$ and for third generation leptoquarks below $148 \text{ GeV}/c^2$. In Figure 2, the decay of the leptoquark to $c\bar{\nu}_\tau$ is limited by the top quark mass, above which the leptoquark will decay preferentially to $t\bar{\nu}_\tau$. When $\Delta M = 0$, $M(\rho_{T8}) < 510 \text{ GeV}/c^2$ for the second generation and $M(\rho_{T8}) < 600 \text{ GeV}/c^2$ for the third generation are excluded at 95% CL.

This analysis reports on the search for leptoquarks produced from continuum and color octet technirho decays in $p\bar{p}$ collisions at $\sqrt{s} = 1.8 \text{ TeV}$ using 88 pb^{-1} of data. Events with two or three jets, substantial missing energy, and no high transverse momentum leptons are subjected to the jet probability requirement indicating at least one jet being consistent with originating from a heavy flavor. No excess of events above Standard Model predictions are found and therefore 95% CL limits are determined.

We thank the Fermilab staff and the technical staffs of the participating institutions for their vital contributions. We

also wish to thank Ken Lane for assistance in deriving technicolor production cross sections. This work was supported by the U.S. Department of Energy and National Science Foundation; the Italian Istituto Nazionale di Fisica Nucleare; the Ministry of Education, Science, Sports and Culture of Japan; the Natural Sciences and Engineering Research Council of Canada; the National Science Council of the Republic of China; the Swiss National Science Foundation; the A. P. Sloan Foundation; the Bundesministerium fuer Bildung und Forschung, Germany; and the Korea Science and Engineering Foundation.

-
- [1] J.C. Pati and A. Salam, Phys. Rev. **D8**, 1240 (1973); J.C. Pati and A. Salam, Phys. Rev. Lett. **31**, 661 (1973); J.C. Pati and A. Salam, Phys. Rev. **D10**, 275 (1973); H. Georgi and S. Glashow, Phys. Rev. Lett. **32**, 438 (1974); E. Farhi and L. Susskind, Phys. Rep. **74**, 277 (1981).
 - [2] L. Abbott and E. Farhi, Phys. Lett. **B101**, 69 (1981); B. Schrempp and F. Schrempp, Phys. Lett. **B153**, 101 (1985).
 - [3] S. Weinberg, Phys. Rev. **D19**, 1277 (1979); L. Susskind, Phys. Rev. **D20**, 2619 (1979); E. Eichten, I. Hinchliffe, K. Lane, and C. Quigg, Phys. Rev. **D34**, 1547 (1986).
 - [4] E. Farhi and L. Susskind, Phys. Rev. **D20**, 3404 (1979).
 - [5] K. Lane and M. Ramana, Phys. Rev. **D44**, 2678 (1991).
 - [6] W. Buchmüller, R. Rückl, and D. Wyler, Phys. Lett. **B191**, 442 (1987).
 - [7] S. Davidson, D. Bailey, and B. Campbell, Z. Phys. **C61**, 613 (1994).
 - [8] J. Hewett and S. Pakvasa, Phys. Rev. **D37**, 3165 (1988).
 - [9] M. Krämer, T. Plehn, and P. Zerwas, Phys. Rev. Lett. **79**, 341 (1997).
 - [10] J. Blümlein, E. Boos, and A. Kryukov, Z. Phys. **C76**, 137 (1997).
 - [11] CDF Collaboration, F. Abe *et al.*, Phys. Rev. Lett. **78**, 2906 (1997); CDF Collaboration, F. Abe *et al.*, Phys. Rev. Lett. **81**, 4806 (1998).
 - [12] D. Acosta and S. Blessing, Annu. Rev. Nucl. Part. Sci. **49**, 389 (1999).
 - [13] DØ Collaboration, B. Abbott *et al.*, Phys. Rev. Lett. **81**, 38 (1998).
 - [14] CDF Collaboration, F. Abe *et al.*, Phys. Rev. **D55**, 5263 (1997).
 - [15] CDF Collaboration, F. Abe *et al.*, Phys. Rev. Lett. **82**, 3206 (1999);
 - [16] CDF Collaboration, F. Abe *et al.*, Nucl. Instr. Meth. **A 271**, 387 (1988); CDF Collaboration, F. Abe *et al.*, Phys. Rev. **D50**, 2966 (1994).
 - [17] S. Cihangir *et al.*, Nucl. Instr. Meth. **A360**, 137 (1995).
 - [18] CDF Collaboration, F. Abe *et al.*, Phys. Rev. **D47**, 4857 (1993).
 - [19] CDF Collaboration, F. Abe *et al.*, Phys. Rev. **D50**, 2966 (1994).
 - [20] CDF Collaboration, hep-ex/9910049, submitted to Phys. Rev. Lett., (1999).
 - [21] CDF Collaboration, F. Abe *et al.*, Phys. Rev. **D53**, 1051 (1996).
 - [22] F. Berends, H. Kuijff, B. Tausk, and W. Giele, Nucl. Phys. **B357**, 32 (1991); W. Giele, E. Glover, and D. Kosower, Nucl. Phys. **B403**, 633 (1993).
 - [23] G. Marchesini *et al.*, Comput. Phys. Commun. **67**, 465 (1992).
 - [24] H. Baer, F. Paige, S. Protopopescu, and X. Tata, hep-ph/9305342.
 - [25] T. Sjöstrand, Comput. Phys. Commun. **82**, 74 (1994).
 - [26] CTEQ Collaboration, J. Huston *et al.*, Phys. Rev. **D51**, 6139 (1995).
 - [27] C. Caso *et al.*, Eur. Phys. J. **C3**, 1 (1998).

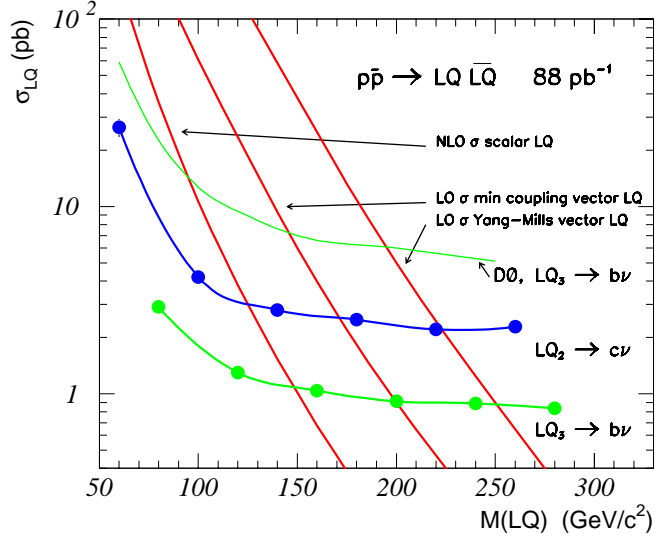


FIG. 1. 95% CL limit for scalar and vector second and third generation leptoquarks assuming $\beta = 0$ compared to theoretical calculations. The D0 Collaboration third generation leptoquark results are also shown [13].

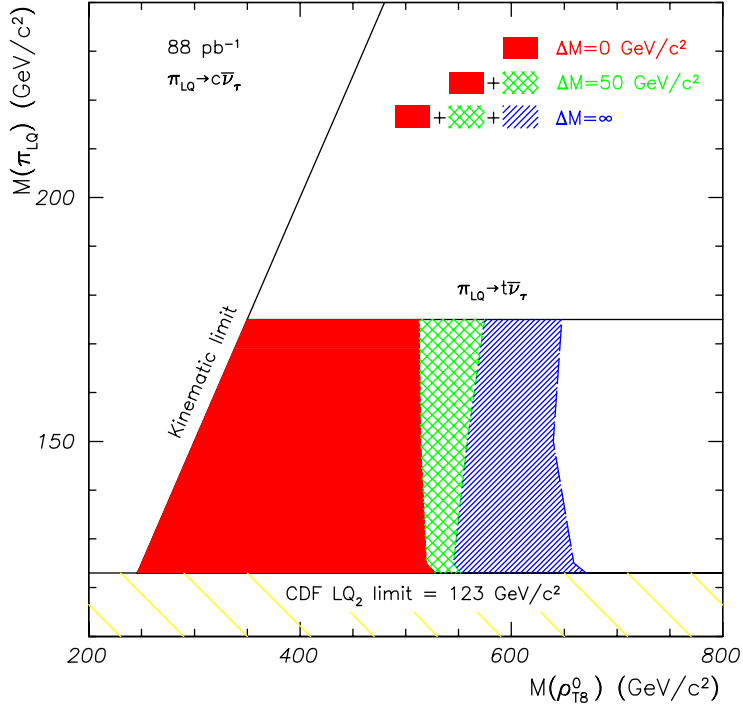


FIG. 2. 95% CL limit for the process $\rho_{T8}^0 \rightarrow \pi_{LQ} \bar{\pi}_{LQ} \rightarrow c \bar{c} \nu_\tau \bar{\nu}_\tau$ at $\sqrt{s} = 1.8$ TeV. The solid region corresponds to a mass difference of $\Delta M = 0$ GeV/c², the solid and hatched regions to $\Delta M = 50$ GeV/c², and all three regions to $\Delta M = \infty$.

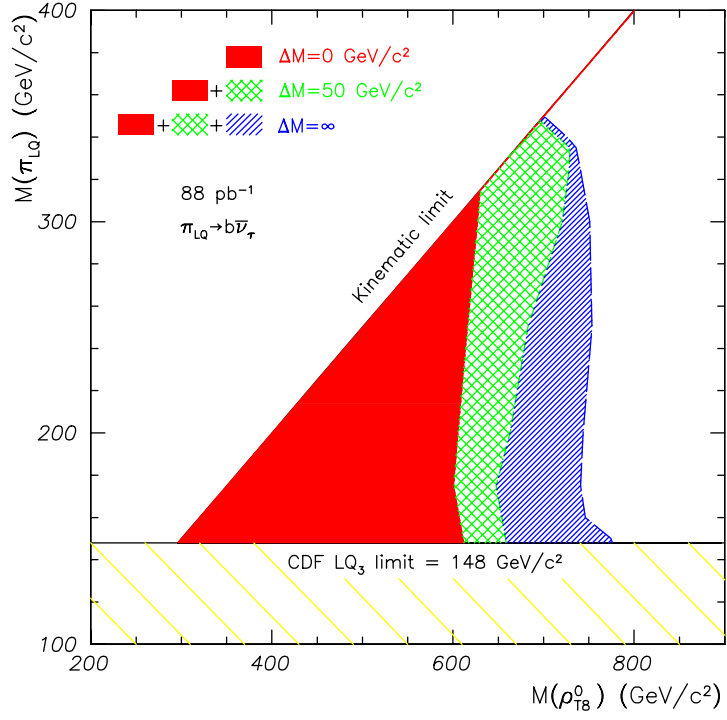


FIG. 3. 95% CL limit for the process $\rho_{T8}^0 \rightarrow \pi_{LQ} \bar{\pi}_{LQ} \rightarrow b\bar{b}\nu_\tau\bar{\nu}_\tau$ at $\sqrt{s} = 1.8$ TeV. The solid region corresponds to a mass difference of $\Delta M = 0$ GeV/c², the solid and hatched regions to $\Delta M = 50$ GeV/c², and all three regions to $\Delta M = \infty$.